Environmental Microbiology

ENVIRONMENTAL MICROBIOLOGY

RESEARCH ARTICLE OPEN ACCESS

Microbial Community Metabolism of Coral Reef Exometabolomes Broadens the Chemodiversity of Labile Dissolved Organic Matter

Zachary A. Quinlan[1] | Craig E. Nelson[2] | Irina Koester[1] | Daniel Petras[3,4] | Louis-Felix Nothias[3,5] | Jacqueline Comstock[6] | Brandie M. White[7] | Lihini I. Aluwihare[1] | Barbara A. Bailey[7] | Craig A. Carlson[6] | Pieter C. Dorrestein[3] | Andreas F. Haas[8] | Linda Wegley Kelly[1]

[1]Scripps Institution of Oceanography, UC San Diego, La Jolla, California, USA | [2]Daniel K. Inouye Center for Microbial Oceanography: Research and Education, Department of Oceanography and Sea Grant College Program, School of Ocean and Earth Science and Technology, University of Hawai'i at Mānoa, Honolulu, Hawai'i, USA | [3]Collaborative Mass Spectrometry Innovation Center, Skaggs School of Pharmacy and Pharmaceutical Sciences, UC San Diego, La Jolla, California, USA | [4]Controlling Microbes to Fight Infections Cluster of Excellence, University of Tuebingen, Tuebingen, Germany | [5]Université Côte d'Azur, CNRS, ICN, Nice, France | [6]Department of Ecology, Evolution and Marine Biology and Marine Science Institute, University of California, Santa Barbara, California, USA | [7]Department of Mathematics and Statistics, San Diego State University, San Diego, California, USA | [8]NIOZ Royal Netherlands Institute for Sea Research and Utrecht University, Texel, the Netherlands

Correspondence: Linda Wegley Kelly (lwegley@ucsd.edu)

Received: 19 July 2024 | **Revised:** 27 January 2025 | **Accepted:** 4 February 2025

Funding: This work was supported by US National Science Foundation, OCE-2023298, OCE-2023509, OCE-2118617, OCE-2118618, GRFP-2019252845; US National Science Foundation, Moorea Coral Reef Long-Term Ecological Research (OCE-1637396). This research was also funded in part by a grant/cooperative agreement from the National Oceanic and Atmospheric Administration, Project A/AS-1; which is sponsored by the University of Hawaii Sea Grant College Program, School of Ocean and Earth Science and Technology (SOEST), under Institutional Grant No. , NA24OARX417C0024-T1-01 from NOAA Office of Sea Grant, Department of Commerce. The views expressed herein are those of the author(s) and do not necessarily reflect the views of NOAA or any of its subagencies. This is Hawaii Sea Grant publication number 4949 and SOEST grant number 11904.

Keywords: coral reefs | dissolved organic matter | exometabolome | marine microbes | molecular networking | tandem mass spectrometry

ABSTRACT

Dissolved organic matter (DOM) comprises diverse compounds with variable bioavailability across aquatic ecosystems. The sources and quantities of DOM can influence microbial growth and community structure with effects on biogeochemical processes. To investigate the chemodiversity of labile DOM in tropical reef waters, we tracked microbial utilisation of over 3000 untargeted mass spectrometry ion features exuded from two coral and three algal species. Roughly half of these features clustered into over 500 biologically labile spectral subnetworks annotated to diverse structural superclasses, including benzenoids, lipids, organic acids, heterocyclics and phenylpropanoids, comprising on average one-third of the ion richness and abundance within each chemical class. Distinct subsets of these labile compounds were exuded by algae and corals during the day and night, driving differential microbial growth and substrate utilisation. This study expands the chemical diversity of labile marine DOM with implications for carbon cycling in coastal environments.

1 | Introduction

Microbial metabolism of marine dissolved organic matter (DOM) has a major influence on the global carbon cycle (Carlson and Hansell 2014). The marine DOM pool stores over 600 Pg of reduced carbon, a reservoir comparable to the amount of carbon dioxide in the atmosphere (Hansell 2013), and the fate of DOM is a key determinant of the metabolic

balance of aquatic ecosystems (Duarte and Cebrián 1996). Fluxes of marine DOM depend on the biological reactivity of various molecules, referred to as lability, determined by the interplay of chemical structure and the metabolic potential of marine microbes (Carlson and Hansell 2014; Azam and Malfatti 2007). Defining the types of molecules that comprise the labile DOM pool is a major question in marine biogeochemistry (Moran et al. 2016).

Coral reefs offer an effective testbed to explore the diversity and lability of marine DOM because dense populations of evolutionary divergent benthic organisms support high primary production that is tightly recycled by diverse microbial communities (Nelson et al. 2023). Previous studies have characterised subsets of coral reef DOM, highlighting differences in production and exudation among a variety of coral and benthic macroalgal taxa in terms of bulk DOC, dissolved combined neutral sugars, fluorescent signatures and solid-phase-extracted pools (Nelson et al. 2013; Haas et al. 2013; Quinlan et al. 2019, 2018). Recent advances in the extraction and analysis of marine DOM pools using high-resolution untargeted mass spectrometry have enabled the identification and differentiation of a greater proportion of these DOM compounds (Dittmar et al. 2008; Wegley Kelly et al. 2022, 2021; Koester et al. 2022; Nothias et al. 2020; Petras et al. 2017). For example, a recent study comparing exudates of corals and algae contrasted higher nitrogen and phosphorus contents in coral DOM with algal DOM exhibiting more reduced nominal oxidation states of carbon, increasing potential energy gained during catabolism (Wegley Kelly et al. 2022). Yet, little is known about the bioavailability of compounds that comprise these complex DOM pools or how the chemical properties of distinct exudate pools influence the metabolism of consumers (Repeta and Aluwihare 2024).

Exudates of coral reef organisms are well established as containing measurable quantities of labile DOM (Brocke et al. 2015) that fosters the rapid growth of ambient microbial communities (Nelson et al. 2023; Haas et al. 2011). Experimental work has demonstrated that fresh exudates of algae and corals elicit distinct microbial communities through differential enrichment of specific heterotrophic taxa (Nelson et al. 2013; Weber et al. 2022), and the general patterns of enrichment have been recapitulated observationally in surveys of coral-dominated and algal-dominated reefs (Haas et al. 2016; Glasl et al. 2019; Apprill et al. 2021; Wegley Kelly et al. 2014). Microbial growth rates and efficiencies have been shown to differ between coral and algal exudates in 1–2 days of incubations (Nelson et al. 2013; Haas et al. 2013), suggesting that the labile DOM components differ between the two organismal classes and consistent with the idea that those labile components are metabolised by different pathways (Haas et al. 2016). Evidence demonstrating significant diel swings in microbial community composition in reefs (Wegley Kelly et al. 2019), when coupled with recent demonstrations of diel differences in DOM production and composition in the day and night (Wegley Kelly et al. 2022; Mueller et al. 2022), points towards significant diel differences in the labile DOM pools exuded by corals and algae on reefs. Together, these discoveries suggest that exploring variation in labile DOM production and composition day and night from benthic primary producers will have implications for organic matter cycling in coastal oceans.

Determining the lability of DOM generated by different coral reef constituents may help resolve how widespread benthic phase shifts from stony corals to fleshy algae alter the reef water chemistry and initiate positive feedback loops that diminish the growth and resilience of reef-building organisms. Coral reef habitats dominated by fleshy macroalgae exhibit elevated microbial concentrations and metabolic shifts towards copiotrophic strategies that alter trophic energy flow, a process termed microbialisation (Haas et al. 2016; McDole et al. 2012). Growing evidence indicates that greater microbial loads on algal-dominated reefs are associated with increased bacterial carbon demand and less efficient catabolic pathways (Nelson et al. 2013; Haas et al. 2016; Roach et al. 2017). This heterotroph-dominated metabolic state results in higher concentrations of opportunistically pathogenic taxa and higher prevalence of coral disease and mortality (Smith et al. 2006; Dinsdale et al. 2008; Mao-Jones et al. 2010). The rates of production and chemical composition of the labile DOM in reefs are likely to be a key regulator of the disrupted nutrient recycling and pathogenesis during microbialisation, and understanding how reefs change in labile DOM production and consumption during phase shifts is crucial for future management (Nelson et al. 2023).

To identify and classify a broader range of labile compounds in marine DOM pools and achieve a better understanding of organic carbon transformation in coral reef environments, we introduced newly produced DOM substrates to marine microbes in dilution culture experiments. The organic exudates (exometabolomes) derived from five common benthic primary producers were characterised before and after a 2-day degradation of bioavailable DOM compounds by resident marine microbes. We tracked the differential growth of microbial communities on the various exudate pools as well as shifts in taxonomic profiles. Our report includes the identification of nearly 200 molecular families comprising more than 1200 ion features that were bioavailable to marine microbes; these exometabolites were putatively classified into compound superclasses spanning eight broad chemical designations and nearly 50 narrow compound subclasses. Distinctions between the amounts of various classes of labile exometabolites were generated by different primary producers translated to differences in microbial community growth rates and taxonomic composition. Finally, this study illustrated differential production and utilisation of labile exometabolites within daytime and nighttime DOM exudate pools.

2 | Methods

2.1 | Organism Collection and Aquaria Design

Two species of reef-building (i.e., skeleton depositing) and zooxanthellate coral (*Pocillopora verrucosa* and *Porites lutea/lobata* complexes), turfing algae, crustose coralline algae (CCA) and the brown macroalgae *Dictyota ceylanica* were collected in Moorea, French Polynesia, between 11 and 14 September 2017 from the backreef lagoon (17°28′55″ S, 149°50′43″) at depths between 2 and 5 m. Organisms were transplanted to a flow-through seawater system at the Richard B. Gump South Pacific Research station within an hour of collection and allowed to acclimate within the flow-through system for a minimum of 2 days underneath shade cloth to reduce irradiance

(Wegley Kelly et al. 2022). Surface area measurements of coral and turf were conducted using calliper estimations and generalised geometric shapes following previously described methods (Wegley Kelly et al. 2022). CCA and *Dictyota* were determined using imageJ; *Dictyota* was wet weighed, dismantled and imaged to estimate the weight-to-surface-area relationship. Organism surface areas were standardised to roughly 1000 cm^2 within each exudation aquaria.

2.2 | Primary Producer Exudation

On 16 September 2017, six polycarbonate aquaria (10 L each) were established adjacent to each other in a single flow-through water table to maintain stable temperature around all aquaria (Figure 1a); one aquarium was established for each of the five benthic primary producer organisms (*Pocillopora, Porites*, CCA, Turfing algae and *Dictyota*) and a sixth aquarium containing only seawater (Control). The six seawater-leached and acid-washed aquaria were filled with 0.22-μm filtered offshore water (collected >1 km north of the forereef of Mo'orea); polyethersulphone filters (SUPOR, Cytiva) were first flushed with 1 L of seawater to remove plasticisers. Exudation aquaria were recirculated using pre-cleaned and leached Rio Aqua 50+ pumps. Aquaria were held at a constant 10-L volume by balancing the inflow and outflow collection of exudate water. Beginning at 06:00/20:00 (day/night, respectively), water was pumped through sample flushed acid-washed platinum cured silicone tubing at 33 mL per minute for an approximate residence time of 5 h; exudates were harvested continuously by outflow pumping flushed 0.22-μm Sterivex filters (Millipore) into acid-washed polycarbonate carboys maintained at ambient temperatures in the dark. Daytime and nighttime exudates were thus harvested continuously over the respective 9-h periods in the day (6:00–15:00 on 16 September) and again at night (20:00–05:00 on 18 September).

2.3 | Microbial Metabolism of Exudates

Dark incubation experiments were used to examine microbial metabolism of exuded DOM. Immediately following the respective daytime or nighttime exudation period, the collected exudates from each of the six aquaria were inoculated to one-third whole ambient backreef water (collected from the same location as the specimens within the 6 h prior to inoculation), mixed and aliquoted within 1 h to four replicate 1-L acid-washed and sample-rinsed polycarbonate bottles, which were stored in a sealed, dark container in a flow-through water table for 48 h. Sampling was initiated within 2 h of inoculation. Flow cytometry samples were collected by pipet (1 mL amended with 16 μL of 32% PFA (EMS), mixed by inversion, snap-frozen) at roughly 0, 4, 8, 16, 24, 32, 40 and 48 post sample inoculation during the incubations of day and night exudates, respectively. At time zero (T_0) and time final (T_F, 48-h), water was harvested for DNA and metabolite measurement via peristaltic pumping. T_0 samples were taken in replicate from each exudate inoculation ($n = 6$) for both daytime and nighttime exudate incubations for a total of 24 T_0 samples. T_F samples were taken from the four replicate dilution cultures for each exudate inoculation and diel cycle for a total of 48 T_F samples. Platinum cured silicone sampling pump lines were flushed with 10 mL of sample followed by a further flushing of 150 mL through 0.22-μm polyethersulphone filter cartridges (Sterivex). After flushing, the filtrate was collected in acid-washed triple-sample rinsed 2-L polycarbonate bottles and acidified to pH 2. Acidified metabolites were further extracted using Agilent PPL cartridges, which had been prepped and activated following (Dittmar et al. 2008). In parallel with the metabolite sampling, the filtrate was additionally collected and analysed for bulk dissolved organic carbon (DOC) (further explained within the Data S1). After sample collection, Sterivex filters were pumped dry with air, PPL cartridges were dried with nitrogen gas, and both the Sterivex filters and PPL cartridges were frozen at −40°C.

2.4 | Enumeration of Microbial Concentrations

Flow cytometry was used to measure total nucleic acid–stained cell concentrations following previously described methods (Quinlan et al. 2019). Samples were thawed, and 200 μL were aliquoted into u-bottomed 96-well autosampler plates and stained with SYBR Green I stain for a final concentration of 1×. Samples were analysed on an Attune Acoustic Focusing Cytometer with Autosampler Attachment (Life Technologies, Eugene, OR, USA). Samples were run at a flow rate of 100 μL min^{-1} on standard sensitivity; 150 μL of sample was aspirated, 75 μL was counted and data were collected only from the last 50 μL (event rates were empirically determined to be steady only after 25 μL of continuous sample injection) (Nelson et al. 2015).

2.5 | DNA Extractions and Sequencing

Microbial DNA was extracted from Sterivex filters using the NucleoSpin Tissue purification kit following the manufacturer's protocol (Macherey-Nagel). We amplified the V3–V4 region of the 16S rRNA gene using polymerase chain reaction following the protocols outlined within (Kozich et al. 2013) and the 341F and 785R primers recommended by (Klindworth et al. 2012). The resultant sequences were analysed with mothur (v. 1.39.5; (Schloss et al. 2009)) following standardised pipelines (described within (Arisdakessian et al. 2020; Jani et al. 2021)). Sequence reads were denoised using DADA2 (Callahan et al. 2019), aligned to the SILVA database (v. 132) and subsequently clustered to a 97% sequence identity operational taxonomic units (OTUs) (VSearch distance-based greedy clustering algorithm; (Rognes et al. 2016)). Sequences were randomly subsampled from each sample at a read depth of 8500 to standardise sampling effort.

2.6 | Untargeted Mass Spectrometry and Molecular Networking

Frozen PPL columns were thawed and DOM was eluted with 2-mL LC–MS-grade methanol, dried via vacuum centrifugation and redissolved in 100-μL MeOH:-water (80:20, LC–MS grade). DOM was analysed using reverse-phase ultra-high-performance liquid chromatography high-resolution tandem mass spectrometry in positive mode on an electrospray injection (ESI) quadrupole-orbitrap mass spectrometer (as described in

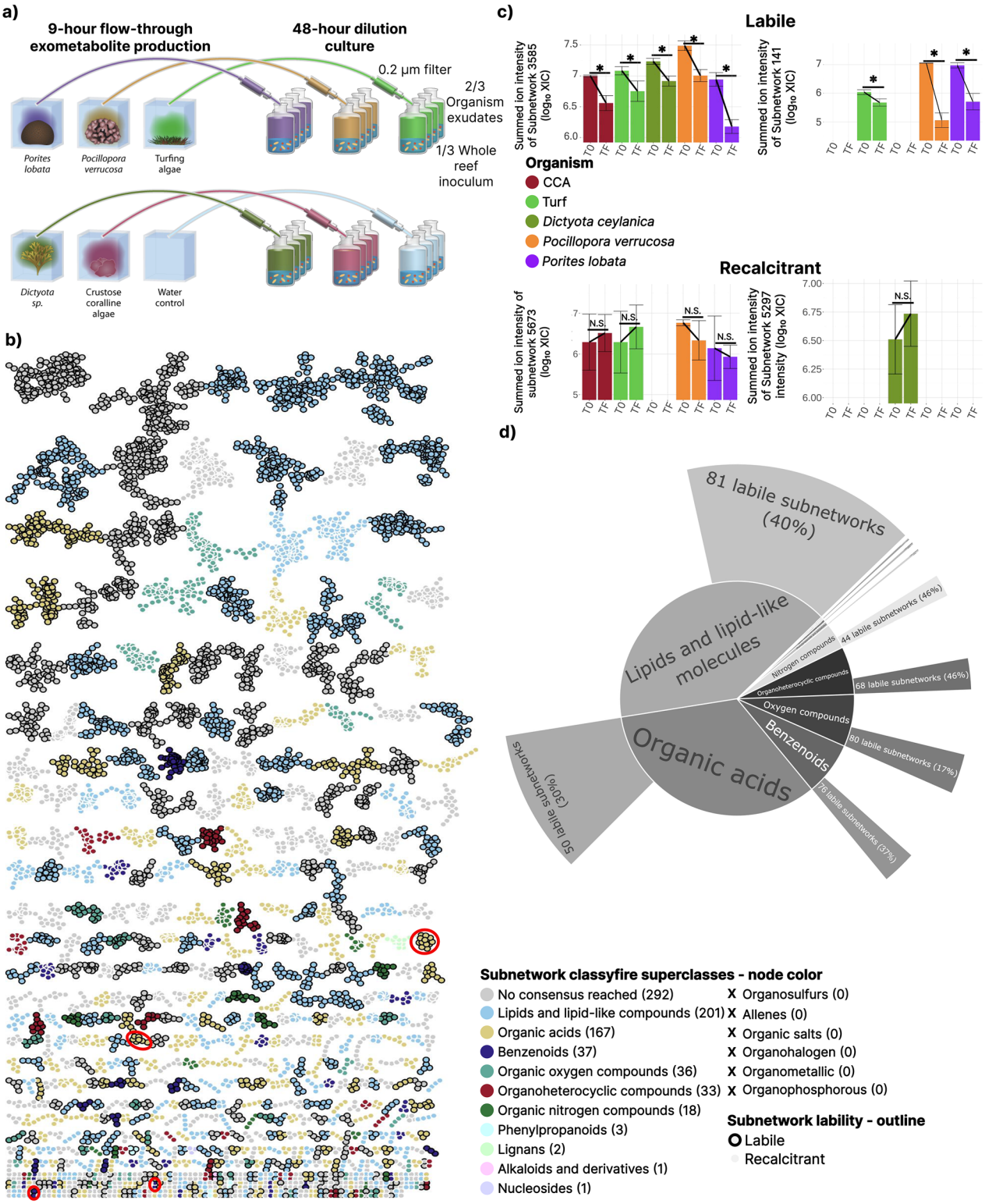

FIGURE 1 | Experimental approaches to characterise the diversity and lability of exometabolites derived from corals and algae. Panel (a) shows the conceptual design of the experiments run both day and night. Panel (b) is a molecular network of all exometabolite features coloured by ChemOnt superclass annotation; subnetworks outlined in black were statistically depleted in 48-h dilution cultures and deemed labile. Subnetworks visualised in panel c are circled in red. Panel (c) illustrates examples of subnetworks that decreased in ion intensity (labile) or remained static (recalcitrant) in 48-h dilution cultures. Panel (d) is a sunburst plot depicting the proportions of subnetworks assigned to each superclass and the percentage that were defined as labile (data detailed further in Table S1). N.S., non-significant.

the Data S1 and Wegley Kelly et al. 2022). Feature-based molecular networking through MzMine 2 (as described in the Data S1 and (Pluskal et al. 2010)) and the global natural product social molecular networking (Wang et al. 2016) was utilised to build a molecular network from all 20,742 features observed within the dataset (Wegley Kelly et al. 2022; Nothias et al. 2020; Wang et al. 2016; Aron et al. 2020; Schmid et al. 2021).

2.7 | Metabolomic Data Curation

Ion features identified using liquid chromatography tandem mass spectrometry (LC–MS/MS) were filtered through a series of four filtering steps both global (applied across all features independent of treatment) and local (applied within treatments; Figure S1). First, two global filters were applied to remove ion features from all samples. First, *Background Features* were classified as those with an average intensity across all samples less than double the maximum intensity of that feature in *Method blanks* (blank water ran through the sampling system in parallel with samples to collect background contamination); (12). Second, *Transient Features* were classified as features with intensities greater than $2*10^5$ (double the defined noise threshold) in fewer than three samples; (12). After both Background ($n=6899$) and Transient ($n=3238$) features were removed from the global dataset, the remaining ion features ($n=10{,}605$) were filtered through specific focusing steps to locally reduce each treatment dataset to abundant exometabolite features as follows (Figure S1). An *exometabolite criterion* was used to classify features as *Organismal Exometabolites* if mean T_0 $\log_{10}$ organism: control was greater than 1, following the conceptual guidance of (Wegley Kelly et al. 2022).

2.8 | Subnetwork Reactivity

Molecular subnetworks, clusters of ion features with high spectral similarity (cosine score ≥ 0.7; 25), were classified based on reactivity by testing if abundant features (maximum intensity >1 SD above the mean) within each subnetwork were, on average, recalcitrant (non-changing) or labile (decreasing abundance). Subnetwork average feature change was evaluated using a linear mixed model to test if abundant ion features within a subnetwork changed significantly on average from starting to ending time points separately in each daytime and nighttime 48 h of incubation, specified as ($\log_{10}$ XIC~Timepoint + (1|Organism) + (1|Feature)), where $\log_{10}$ XIC is the base 10 logarithm of the feature peak area or extracted ion chromatography intensity; to evaluate relative rather than absolute change, intercepts were allowed to vary among each feature (Feature) in each exudate treatment (Organism). Labile exometabolite features were defined as those abundant exometabolites belonging to labile subnetworks; because individual ion features were classified separately for each of the six treatments, the subset of labile exometabolites differs in each treatment (Figure S1).

2.9 | Ion Feature Annotation

Elemental composition and putative compound classes were predicted for each feature using SIRIUS 4. Molecular formulas were predicted using SIRIUS and reranked within the ZODIAC workflow (Ludwig et al. 2020, 2018). Compound classes based on ClassyFire from ChemOnt ontologies were predicted using the CANOPUS workflow (Dührkop et al. 2021). Molecular spectra were given library and analogue annotations by spectral matching against public and commercial libraries via the feature-based molecular networking (Wegley Kelly et al. 2022; Nothias et al. 2020) workflow with cosine similarity thresholds of 0.7 and 0.8, respectively. Next, we utilised molecular subnetworks, defined within FBMN as clusters of paired ion features with high spectral similarity (cosine score ≥ 0.7). By leveraging the ability of subnetworks to cluster compounds of similar spectral characterisation, we established putative consensus annotations through the comparison of node annotations within the subnetworks using the ConCISE framework using CANOPUS predicted chemical classes (Quinlan et al. 2022).

2.10 | Statistical Analyses

All post-processing of exometabolite intensity, bacterial cell growth and microbial community composition was analysed using in-house-written R pipelines (using Tidyverse, data.table, DescTools, readxl, CHNOSZ, ggpubr, vegan, ape, RColorBrewer; (Wickham, Averick, Bryan, et al. 2019; Dowle et al. 2019; Signorell et al. 2019; Wickham, Bryan, Kalicinski, et al. 2019; Dick 2019; Kassambara and Kassambara 2020; Dixon 2003; Paradis et al. 2004; Neuwirth and Neuwirth 2011)), which are openly available on Github (github.com/zquinlan/DielReefEnrichments). Sequence reads were converted to relative abundance within each sample and filtered to only those OTU's that were either abundant ($>5.0\%$ abundance in a single sample) or prevalent (abundance $>0.1\%$ in at least three samples). OTUs were curated to only those that had a higher relative abundance in at least one organism treatment above the water control, prior to running any statistics. To capture the dynamic portions of the microbial community, a non-parametric, two-way permutational analysis of variance was utilised to contrast OTU abundance between both organism and diel treatments (relative abundance~Organism*Diel).

The specific growth rate of microbial communities was calculated as $(\ln(\text{cell}_{max})-\ln(T_0))/T_{max}$, where the cell_{max} was calculated at the timepoint when the microbial load peaked as each community exhibited independent growth curve dynamics (Figure S2). Before statistical analysis, all ion feature intensity was transformed to approximate a Gaussian distribution ($\log_{10}$). Microbial relative abundances were unable to be transformed to approximate Gaussian distributions because the data are inherently 0 biased; all microbial data were analysed with non-parametric analyses. Microbial and metabolomic dynamics were contrasted between coral and fleshy algae using a linear mixed model controlling for organism as a random effect, excluding CCA (response variable~organism type*diel + (1|Organism); Figure 6). All p values reported were FDR-corrected (Benjamini and Hochberg 1995). The Bray–Curtis dissimilarities of summed consensus subclasses were used for the metabolite PCoA shown in Figure 5. Weighted Unifrac distances were used for microbial composition PCoA shown in Figure S3a,b.

3 | Results

3.1 | Production and Measurement of Coral Reef-Derived Exometabolites

To generate freshly produced DOM in coral reef waters, organic exudates were separately harvested both day and night from five benthic primary producer taxa prevalent across the reefs in Mo'orea, French Polynesia: Two species of hermatypic coral (*Pocillopora verrucosa* and *Porites lutea/lobata* complexes), one crustose coralline algae (CCA, *Hydrolithon reinboldii*), one brown macroalgae (*Dictyota ceylanica*) and a mixed assemblage of turfing algae (Figure 1a). Bulk DOC production ranged between 76.76 and 97.27 μm C in the day and 80.03 and 94.37 μm C in the night (Figure S2). There was a significant difference between organism treatment bulk DOC (two-way ANOVA Organism p value ≤ 3.34*10^−5), but there was no significant drawdown between timepoints (two-way ANOVA Timepoint p value > 0.05) or interaction of timepoint and organism (two-way ANOVA Organism*Timepoint p value > 0.05). After tandem mass spectral analysis (LC–MS/MS) of solid-phase-extracted DOM pools, a total of 10,605 unique ion features were retained after removing features present in process blanks and transient ion features (Figure S1). Roughly one-quarter of these features, 3693 during the day and 3511 at night, were statistically identified as abundant exudates of one or more benthic primary producers (i.e., exometabolites, as described by Wegley Kelly et al. 2022; 12; Figure S1). Each benthic producer released a minimum of 400 exudate features either day or night, with *Dictyota* releasing the most (nearly 1500 features during the daytime incubations); these numbers are consistent with previous exudation experiments (Wegley Kelly et al. documented 1667 exudate features total from similar benthic organisms with more than 400 features released from any organism in a single incubation; 12).

3.2 | Defining Bioavailability of Primary Producer Exometabolites

To determine the bioavailability of exometabolites to reef microbes, samples for DOM composition were collected at the start and end of replicated 48-h dilution cultures (Ammerman et al. 1984; Hagström et al. 1984) where each filter-sterilised exudate pool was inoculated with ambient reef microbes at a 2:1 ratio, respectively (Figure 1a). Structurally similar ion features were clustered to form molecular families or subnetworks (Figure 1b) using the Global Natural Products Social Molecular Networking (GNPS; 42) platform (Nothias et al. 2020; Wang et al. 2016; Schmid et al. 2021). Each molecular family subnetwork was assigned a putative consensus hierarchical annotation (Superclass, Class, Subclass from the ChemOnt chemical ontology; (Djoumbou Feunang et al. 2016)) based on secondary ion fragmentation pattern database identifications and in silico structural predictions utilising the ConCISE framework (Dührkop et al. 2021; Quinlan et al. 2022). A total of 3250 abundant exometabolite features (2569 day and 2044 night, Figure S1) clustered into 1856 subnetworks or molecular families (Nothias et al. 2020; Wang et al. 2016), of which roughly half (1145) were single-feature subnetworks (single loop nodes). Roughly one-quarter of the subnetworks were classified (525). The largest proportions of classified subnetworks were assigned either as lipids (25.4%) or as organic acids (21.1%), with smaller proportions of heterocyclics, oxygen, nitrogen or benzenoid superclasses (2.3%–4.7%); less than three subnetworks each were classified as phenylpropanoid, lignin, nucleoside or alkaloid superclasses.

A central question of this research was to determine what proportion of these molecular families (subnetworks) are bioavailable and whether those that are readily metabolised tend to be associated with just a few of the broad categories of chemical superclasses. The reactivity of each molecular subnetwork in each benthic exometabolite treatment pool was defined as labile or recalcitrant based on the consistency of the change in the mean ion feature intensity from start to end of the 48-h experiment (Figures 1c and S1; linear mixed model FDR $p < 0.05$). Roughly one-quarter of the subnetworks were characterised in this manner as being labile (529%, or 27%), comprising 1180 (36%) of the exometabolite ion features (similarly, one-quarter of the subset of single loop nodes were labile: 274 of 1145). Labile exometabolite subnetworks were found distributed evenly across diverse chemical superclasses (Figure 1c); averaged across day and night exudation experiments, more than 30% of the subnetworks in the lipid, heterocyclic, and nitrogen superclasses were labile, with at least 15% of the subnetworks and ion features statistically labile in each of the other superclasses (Table S1).

3.3 | Daytime Exudation of Broad Chemical Classes of Labile Exometabolites From Reef Organisms

The total quantity (ion intensity) of exometabolites in the daytime was variable among the five organisms (Figure 2a; one-way ANOVA $p = 0.006$). The proportion of the exometabolites classified as labile was similarly variable across the organisms, ranging from 50.7% to 64.6% of the summed ion intensity and varying up to 13.9% among organisms (Figure 2a). Aggregating subnetworks at the broadest chemical classification (superclass), we found significant differences in the overall composition of labile DOM released in the day by each benthic primary producer in both proportional ion intensities (Figure 2b; PERMANOVA, $p = 0.0010$) and total ion intensities (Figure 2c; PERMANOVA, $p = 0.0012$). Qualitative compositional differences indicated that both species of corals and the fleshy algae *Dictyota* labile exometabolite pools were dominated by organic acids during the day (40%–62% of total ion intensity), with turf dominated by organoheterocyclic compounds (53%) and CCA dominated by organic nitrogen compounds (52%; Figure 2b). We found significant quantitative differences among organisms in the total ion intensity of labile exometabolites released in the daytime of four of the six dominant superclasses (Figure 2c; Tukey *post hoc* alpha = 0.05): organic acid production was different among each producer, CCA produced significantly less labile benzenoids, organic acids and lipids than the other producers, and the coral *Porites* produced significantly less organic nitrogen compounds than all other organisms. No significant differences were found among organic oxygen compounds or organoheterocyclic compounds (Figure 2c).

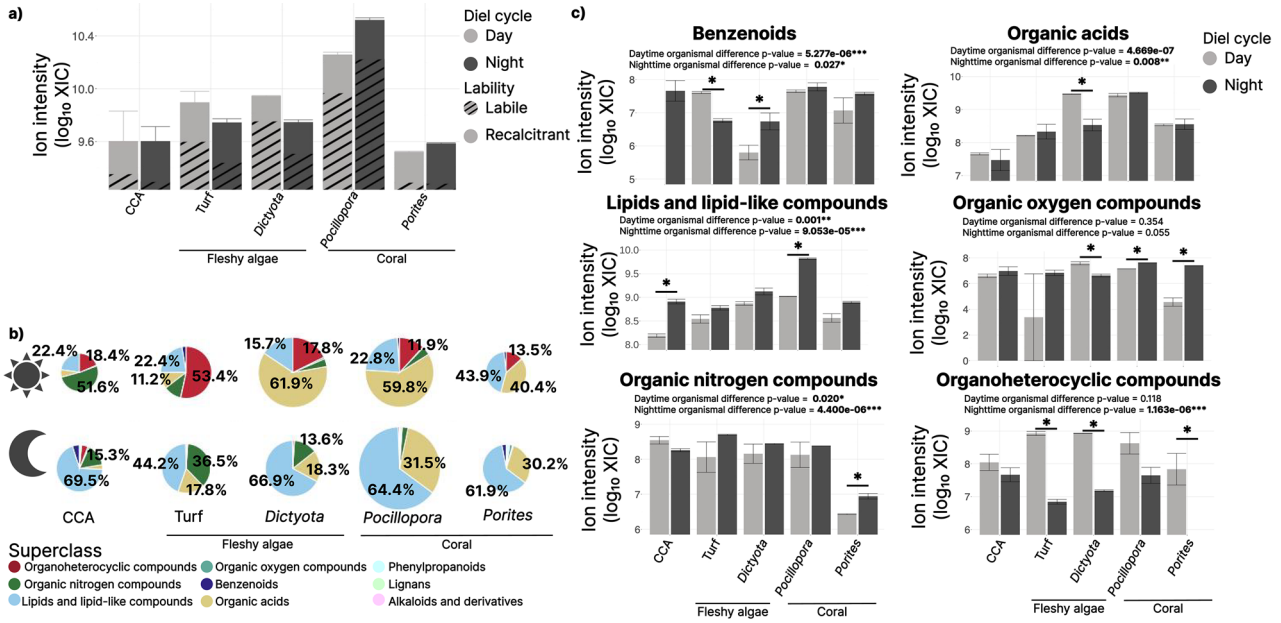

FIGURE 2 | Amounts and superclass composition of labile exometabolites released from coral reef benthic primary producers. Panel (a) shows the mean summed ion intensity of exometabolites in the day and night and the proportion belonging to labile subnetworks. Panel (b) depicts the ion intensity proportions (pie slices) and total amount (pie size) of labile exometabolites annotated to each superclass. Panel (c) illustrates the mean ion intensity of labile exometabolite features from each organism day and night within each superclass. ANOVA *p* values comparing organism means are noted for daytime and nighttime exudate pools. Asterisks denote pairwise diel differences by the Tukey post hoc testing. All bars denote the mean of technical replicates, and whiskers are standard errors of the mean.

3.4 | Contrasting Day and Night Production of Broad Classes of Labile Exometabolites From Reef Organisms

Similar to patterns in daytime labile exometabolite production, the total ion intensity of exometabolites at night was significantly different among the five organisms (Figure 2a; one-way ANOVA $p < 0.001$). In contrast to daytime exudation, the proportion of the exometabolites classified as labile was less variable across the organisms, ranging from 49.5% to 58.1% of the summed ion intensity and never varying more than 8.6% among organisms (Figure 2a). We explored the hypothesis that various reef benthic producers alter the composition of their labile exudates on a diel basis by comparing the proportional and absolute concentrations of labile superclasses during day and night exudations. As with daytime exudation, there was a significant difference between the nighttime organismal production of superclasses both proportionally (Figure 2b: PERMANOVA $p < 0.001$) and by total ion intensity (Figure 2c: PERMANOVA = 0.001). Qualitatively, there was a consistent increase in the proportional lipid production across all organisms tested at night (to 44%–70% of labile DOM), with a corresponding reduction in proportions of organoheterocyclic compounds (less than 5%; Figure 2b). These patterns were reinforced in quantitative data with significant overall diel shifts and diel changes in organismal production via two-way ANOVA (diel and diel:organism $p < 0.05$; Figure 2c). Heterocyclics particularly decreased at night in both fleshy algal and *Porites* treatments, while lipids particularly increased in *Pocillopora* and CCA ($p \leq 0.05$; Figure 2c). There were a few notable day–night shifts in the production of individual labile superclasses, particularly by fleshy algal taxa: Benzenoids were differentially enriched between the fleshy algae, with *Dictyota* enriched at night and Turf enriched in the daytime, and the *Dictyota* treatment showed a diel change in organic acids, significantly enriching them during the day ($p < 0.05$; Figure 2c).

3.5 | Differential Removal of Labile Organismal Exometabolites Between Day and Night

We next tested the hypothesis that the microbial metabolism of labile exometabolites would differ among organismal exudate pools and between day and night exudates. To examine the microbial transformation of labile exometabolite pools produced by different reef organisms, we compared the mean summed ion intensity (XIC) of all depleted exometabolite subnetworks from each replicate incubation bottle at the initial ($n = 2$) and final ($n = 4$) timepoints (Figure 3a). The magnitude of both daytime and nighttime labile exometabolites removed by microbes over the 48-h incubation was similar between treatments, except for the *Pocillopora* treatment where significantly more of the ion intensity was removed from labile subnetworks at night (Figure 3a; Tukey adj. $p < 0.05$). Small diel differences in the microbial removal of labile exometabolite pools were found in CCA, where significantly more labile DOM was removed in the daytime, and in both coral species, where significantly more labile DOM was removed at night; no diel differences in labile DOM removal were observed in either of the fleshy algae (Figure 3a).

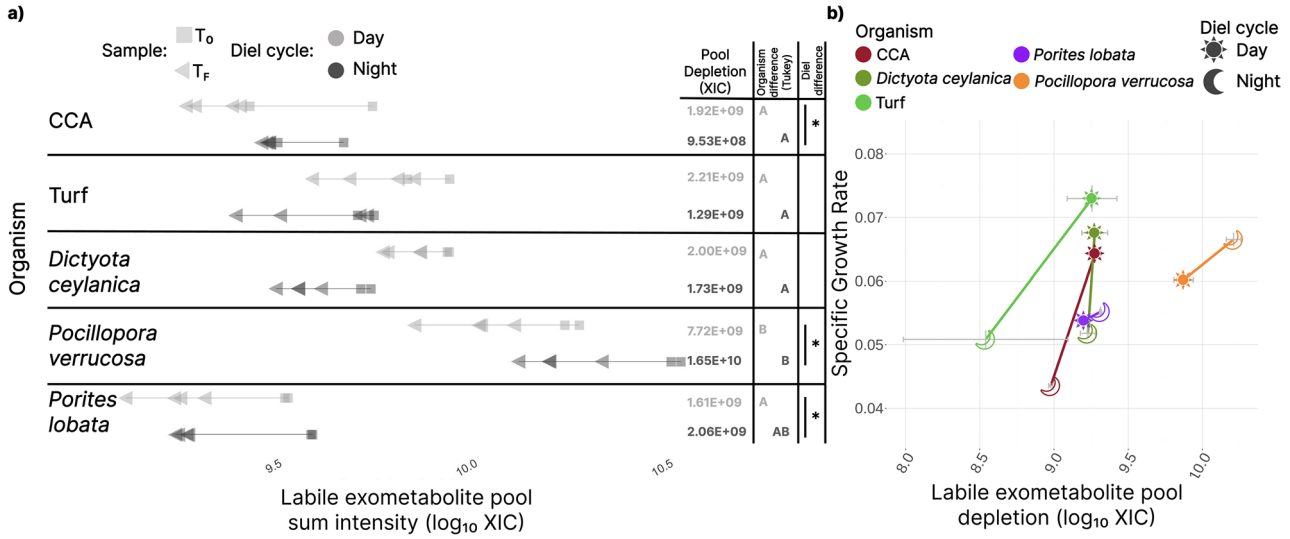

FIGURE 3 | Microbial utilisation of labile exometabolites released from corals and algae. Panel (a) shows the summed XIC from labile exometabolite features in each bottle at the start (squares, $n = 2$) and end (triangles, $n = 4$) of each incubation. The right panel is annotated with the pairwise post hoc testing of differences between organisms (connecting letters) and day vs. night within each organism (asterisks) at alpha = 0.05. Panel (b) demonstrates a significant regression (linear model $p < 0.05$) between the mean labile exometabolite utilisation (from right side of panel a) and mean microbial community specific growth rates in each treatment day and night (see Figure S2 for additional analyses).

3.6 | Differential Microbial Growth on Day and Night Exometabolite Pools Among Corals and Algae

Past work has demonstrated greater microbial community growth rates and higher cell yields on algal exudates than coral exudates (Nelson et al. 2013; Haas et al. 2013), but those exudates were not generated in continuous flow-through conditions as was done here. To understand how microbial communities grow differentially on exometabolites, we tracked cell abundances using flow cytometry roughly every 5–10 h over the 48-h incubation period (Figure S3). Both mean specific growth rates (calculated over the 24-h exponential growth period) and peak cell yields (at 24 h) differed significantly among exometabolite pools both day and night (ANOVA $p < 0.001$; Figure S3a) and were always significantly greater than water controls (Dunnet's post hoc test, $p < 0.001$). The highest specific growth rates on daytime exudates were found in algae (*Dictyota* 1.62 day^{-1}, turf 1.75 day^{-1}, CCA 1.54 day^{-1}), with rates in coral treatments (*Pocillopora* 1.44 day^{-1}, *Porites* 1.29 day^{-1}) significantly lower. Nighttime incubations had significantly lower growth rates and yields than daytime incubations in all three algal exometabolite pools ($p < 0.001$; *Dictyota* 1.24 day^{-1}, Turf 1.22 day^{-1}, CCA 1.04 day^{-1}), whereas *Pocillopora* exudate-enriched microbial communities grew faster at night ($p = 0.0068$; 1.60 day^{-1}) and there was no significant diel change in microbial growth on exometabolites of *Porites* ($p > 0.05$; 1.32 day^{-1}).

To investigate the degree of influence of the labile exometabolites observed within this experiment on microbial community growth, we tested if the total labile exometabolite consumption predicted the microbial specific growth rate among the various organismal and diel pools (Figures 3b and S3b). Across all experiments, labile exometabolite depletion was correlated with specific growth rate ($p = 0.0005$, Figure 3b). This correlation was clear and consistent across the coral incubations ($p = 0.0007$), with increased growth rates and labile exometabolite removal of night exudates but was not significant in the algal exometabolites ($p = 0.054$), where elevated daytime growth rates were not associated with a measurable increase in exometabolite removal (Figure 3b). There was no significant correlation between total labile exometabolite utilisation and specific growth rates within the daytime exometabolite pools ($p = 0.38$; Figure S3b); labile pool total depletion explained 61.6% of the variance in specific growth rate in the two coral treatments ($p = 0.0129$) but not among the three algal species ($p = 0.561$). In contrast, nighttime exometabolite drawdown explained 47.1% of the variation in specific growth rate across all coral and algal organismal treatments (p value = 0.0005; Figure S2b). Taken together, these results point toward the coupling of labile DOM utilisation and microbial growth on both night and day coral exometabolites, whereas microbial growth on the algal exometabolites was uncoupled during the daytime. We predict that this pattern was fuelled by labile substrates produced by benthic algae that fall outside of our analytical window (i.e., compounds with low binding to the PPL resin or outside of our mass range).

3.7 | Microbial Community Differentiation During Growth on Coral Reef Exometabolites

To test the hypothesis that labile exometabolites drive shifts in the microbial community composition (e.g., 7, 20), taxonomic profiles were collected from each bottle at the start and end of each dilution culture. In daytime exometabolite incubations, the composition of the microbial communities in all benthic exometabolite treatments changed significantly more than in the water control over the course of the dilution culture experiment (Figure S4; Mann–Whitney U of weighted unifrac distances p value < 0.00067), demonstrating a community shift in response to

labile exudates. After 48 h, the microbial community structure exhibited distinct associations with the daytime organismal exudate pools that facilitated their growth (Figure 4; Table S2). Coral treatments enriched for *Thallasobius* (Rhodobacteraceae), NS9 marine clade (Flavobacteriales), OM60 (Halieaceae) and an unclassified OTU within the family Rhodobacteraceae (Figures 4 and S4c, Table S2). Fleshy algal exudates enriched for an unclassified OM43 (Methylophilaceae) and *Donghicola* (Rhodobacteraceae; Figure 4). Although Figure 4 contrasts fleshy algae with corals, all algal exudates, including CCA, additionally enriched for *Nautella* (Rhodobacteraceae) and an unclassified OTU within the family Cryomorphaceae (Flavobacteriales). Daytime treatment community evenness on fleshy algae (Peilou's evenness 0.542 ± 0.120; Figure S4c) was significantly lower than on the *Pocillopora* and *Porites* corals (Tukey FDR p value ≤ 2.3e-6; Figure S4c), indicating more selective enrichment of a subset of taxa on algal exometabolites relative to corals.

In the fleshy algae treatments, nighttime microbial composition shifts exhibited a reduced response to exometabolites, consistent with the dampened growth rates relative to daytime exometabolites. Over the course of the dilution culture experiment, only the microbial communities of the two corals and CCA changed significantly compared to the water control (Figure S4b; Mann–Whitney U of weighted unifrac distances p value < 0.00216), whereas the fleshy macroalgae (*Dictyota*) and Turf treatments did not engender a strong microbial community response (Mann–Whitney U of weighted unifrac distances p value = 0.8518). The nighttime microbial community in both coral treatments became dominated by a single strain of Rhodobacteraceae (unclassified beyond family level resolution), which was specific to the night treatment. Because this taxon became so prevalent in the cultures, community evenness in the night treatment was diminished from 0.638 to 0.303 in *Pocillopora* and from 0.640 to 0.422 in *Porites* (Figure S4c; two-sided t-test p value ≤ 0.00294). The three algae communities were not substantially permuted between day and night exometabolite treatments, with the most prevalent taxon represented by the same Cryomorphaceae but at a lower magnitude at night (Figure 4; Table S2), indicating that nighttime algal exometabolites conferred less selective pressure on the microbial community composition than the daytime labile exometabolites.

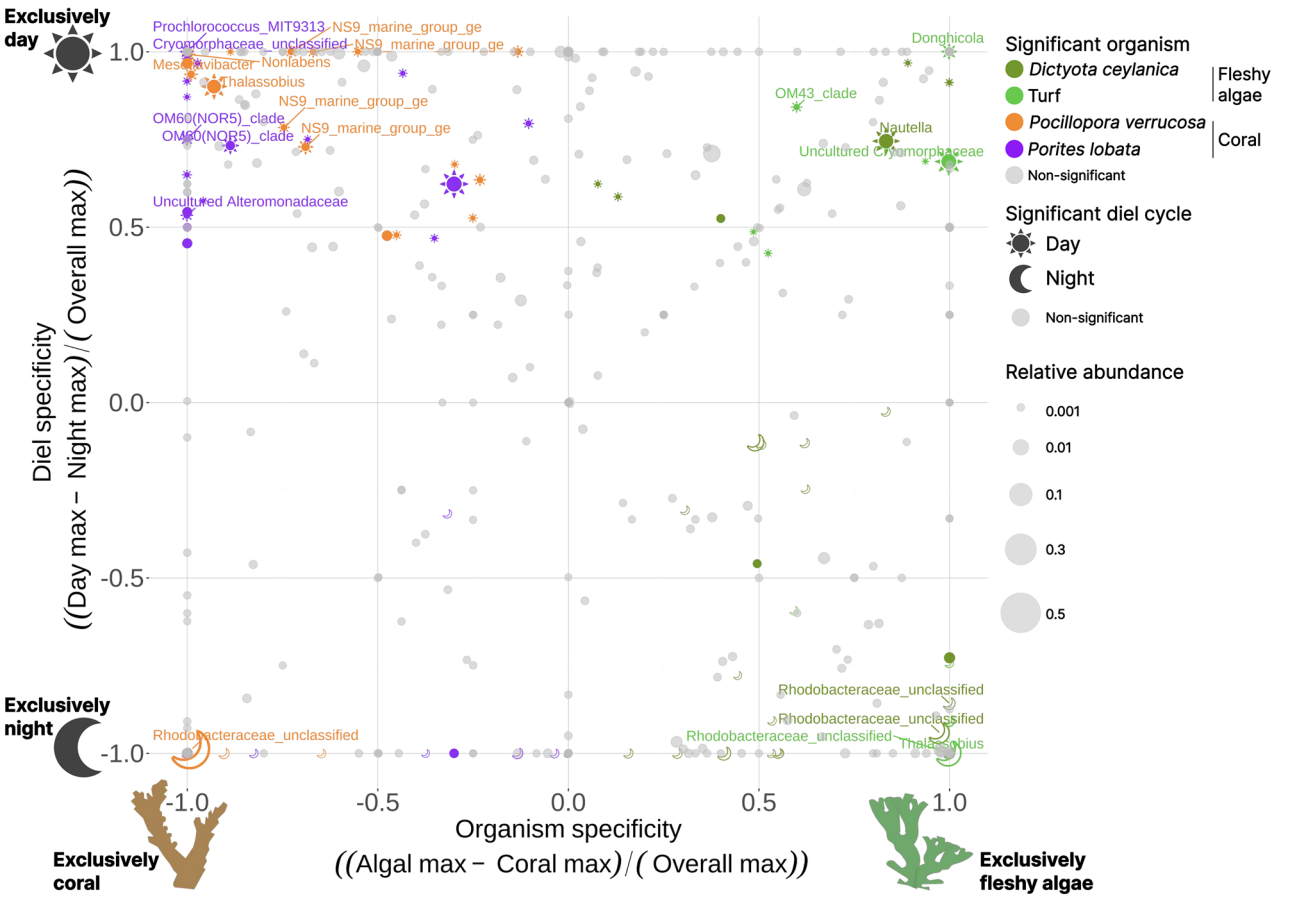

FIGURE 4 | Differential enrichment of specific microbial taxa on daytime and nighttime exudates between corals and fleshy algae. Both x and y axes range from −1 to 1 corresponding to exclusive enrichment by coral or algae (x-axis) and by nighttime or daytime exometabolites (y-axis). Relative selectivity calculated from relative abundances of operational taxonomic units (OTUs). Microbial taxa are coloured if the taxon had a significant effect of organism or diel interaction from a two-way ANOVA. Microbial taxa are shaped as sun or moon if the taxa had a significant effect of diel cycle or organism interaction. All non-significant taxa are conversely plotted as grey circles. All points are sized by the mean relative abundance of the identified treatment and denoted by taxonomic designation if the mean relative abundance was greater than 0.3 in any one treatment or above 0.01 with an organism specificity value (x-axis) greater than 0.5 or less than −0.5.

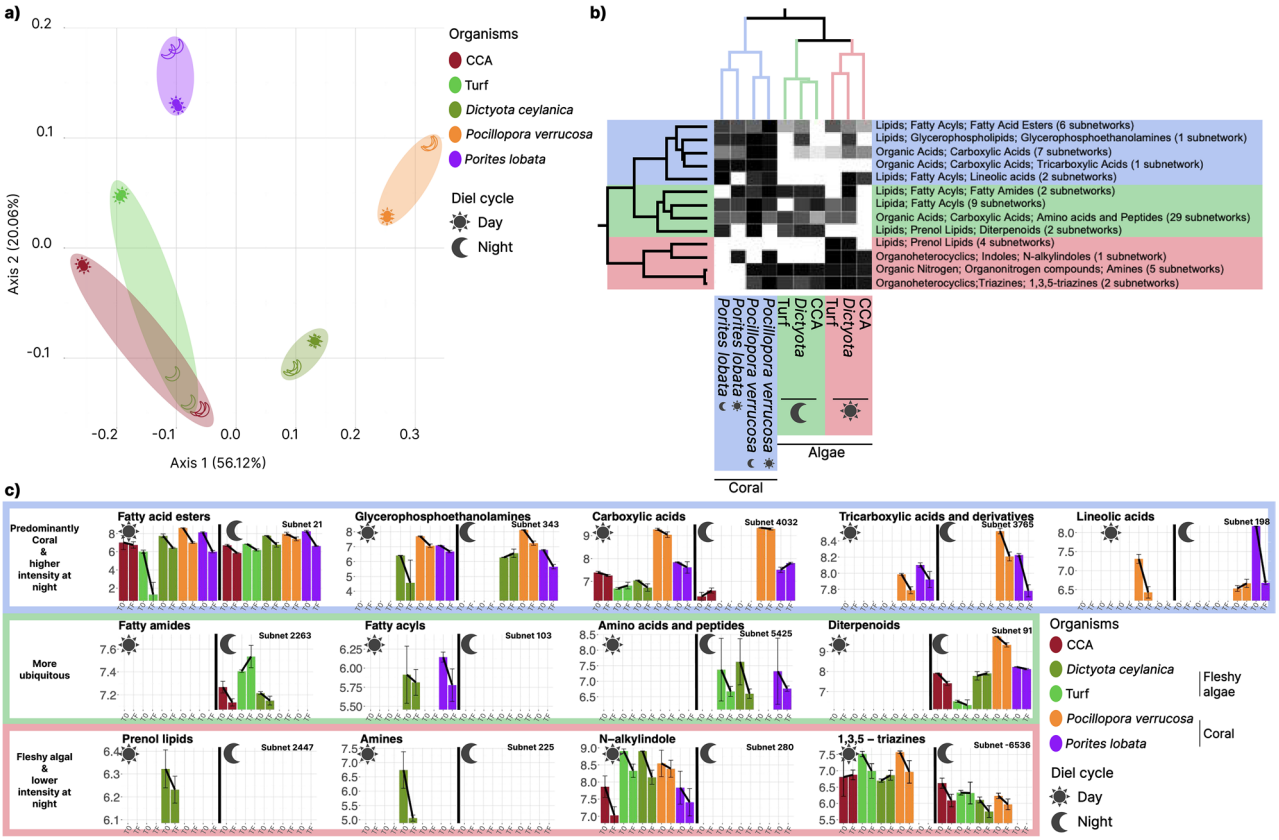

FIGURE 5 | Chemical subclasses of labile exometabolites differ between corals and fleshy algae with greater diel shifts in algal exudates. Panel (a) uses non-metric multidimensional scaling to depict replicate labile exometabolite pools of each organism in the day and night according to the ion intensity of chemical subclasses. Panel (b) uses hierarchical clustering of 13 selected labile exometabolite at the subclass level to illustrate drivers of the pattern in panel (a). The subclasses shown in panel (b) were those annotated to at least class level and quantitatively above average abundance (average XIC greater than $2e^7$ or the 50% quantile of mean XIC across exometabolite pools). Ion intensities (XIC) were standardised (z-scored) and clustered with Ward's minimum variance method using Euclidean distances. Panel (c) shows the raw labile exometabolite intensities from subnetworks representative of the subclasses shown in panel (b).

3.8 | Differential Composition of Labile Coral Reef Exometabolites Between Day and Nighttime

The overall shifts in the bulk labile exometabolite production and diel variability among benthic producers were further resolved by exploring more granular compositional shifts in the labile exometabolite pools. Although the coral reef organisms within this experiment produced labile compounds within the same superclass structural families (Figure 2), the quantity and composition of subnetworks within these categories were much more variable (Figures 5 and S5). To identify specific types of labile exometabolites released by corals and algae during daytime and nighttime on tropical reefs, we examined the characteristics of the 178 subnetworks that were successfully annotated by ConCISE (out of 529 total labile subnetworks) belonging to 48 distinct compound types at the subclass level of the ChemOnt ontology (Figure S5). We visualised patterns in the abundance of these labile subclasses using multidimensional scaling (Figure 5a) and PERMANOVA, quantifying significant differences in multidimensional subclass composition among organisms ($p \leq 0.002$) as well as between the two corals and two fleshy algae ($p \leq 0.009$, daytime $r^2 = 0.34205$, nighttime $r^2 = 0.46272$; Figure 5a). We also observed a significantly smaller diel shift in the labile exometabolite pools of the two coral species than in the three algal species (Figure 5b). Together, these more granular compositional results are consistent with organismal and diel differences in both total labile exometabolite production (Figure 2a) and superclass labile exometabolite production (Figure 2b,c). The differences between corals and algae and day and night qualitatively mirror patterns in labile exometabolite removal (Figure 3a) as well as microbial responses (Figures 3b and 4), demonstrating a greater diel variance in algae than in corals (Figure 5a).

We resolved a suite of chemical subclasses of varying specificity to the exometabolite pools from the various reef organisms: some subclasses only released by one or two organisms, some released more by corals vs. algae and some released widely but in different amounts by each organism. We predicted that some of these compounds would be preferentially released during the day or night in certain benthic producers. Indeed, of the 48 labile exometabolite subclasses, roughly one-third (Brocke et al. 2015) were unique to a single organism (Figure S5). Two subclasses (each comprising a single subnetwork) were produced consistently both day and night by just one organism: Terpene lactones (prenol lipids) by *Dictyota* and alcohol/polyols (organooxygen compounds) by CCA, suggesting that these may be unique to those organisms. Another 16 were produced in only one diel

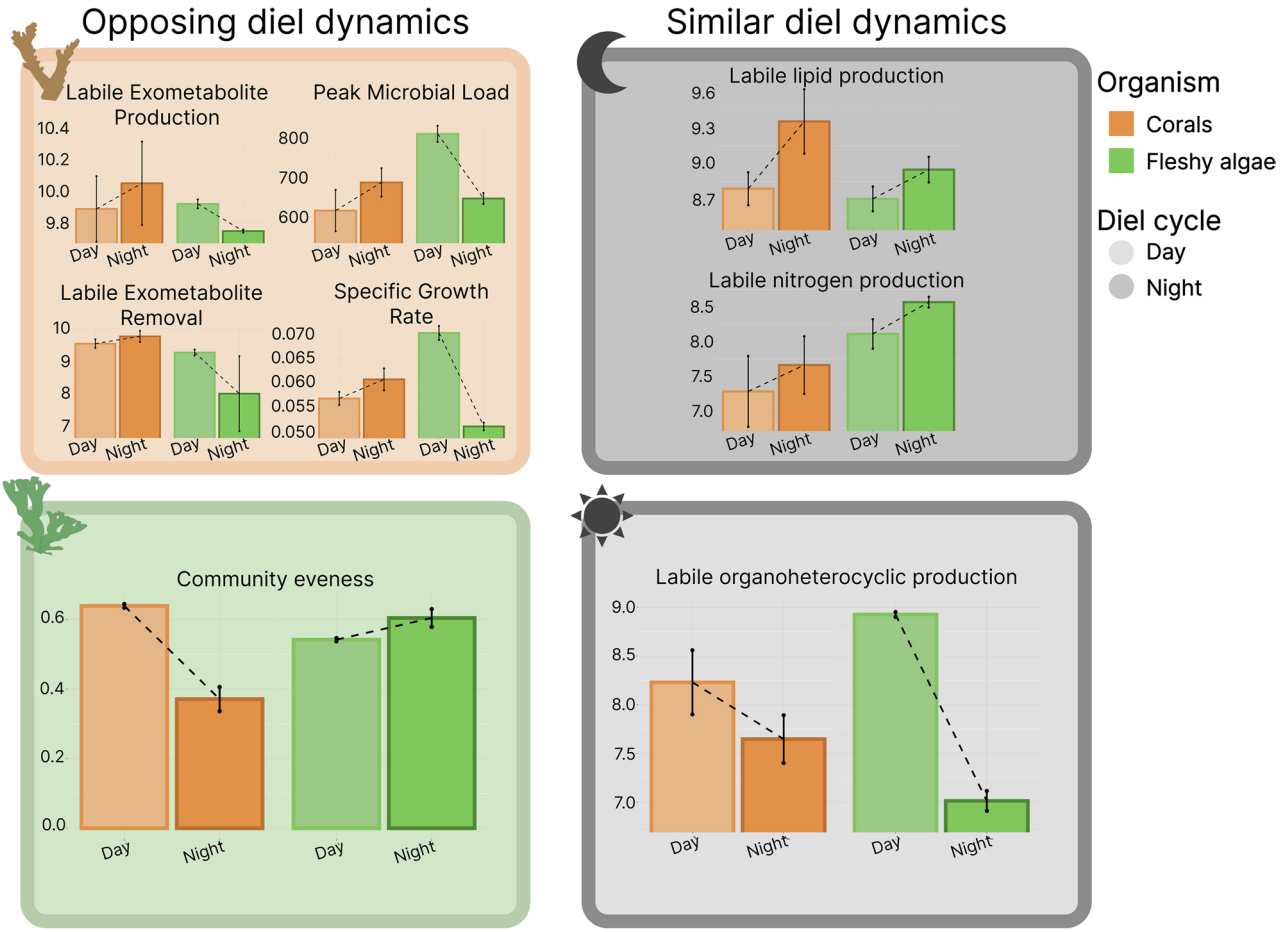

FIGURE 6 | Corals and fleshy algae exhibit consistent diel differences in labile exometabolite production and microbial utilisation that drives differential microbial community shifts. Each response metabolite and microbial community metric is grouped based on whether coral and fleshy algae change similarly (e.g., both increase) or in opposingly (e.g., coral increases, fleshy algae decrease) between night and day. For the opposing dynamics (left), a cartoon version of coral or fleshy algae indicates which organism treatment increased at night. For the metrics that changed similarly, a cartoon sun or moon indicates during which diel period each metric was highest.

period by one organism, including 4 each from CCA, *Dictyota* and *Pocillopora* at night and another 4 by just a single organism in the day (Figure S5). These subclasses that were uniquely produced by single organisms at specific times almost all comprised just one molecular family/subnetwork and were spread evenly across five of the six main superclasses (there were no unique organonitrogen compounds). There were no unique compounds released by Turf or CCA, consistent with our understanding of the cryptic diversity of these tissue types that may include small amounts of macroalgae and other epiphytes. Taken together, these results point to considerable specificity in compound classes comprising the labile exometabolite pools of coral reef primary producers.

The results from this study also reveal the existence of widespread labile exometabolite classes in reefs that are differentially enriched among the exudates of various benthic primary producers day and night. Of the 30 labile exometabolite subclasses that were produced by more than one organism, roughly half (Petras et al. 2017) differed significantly among the various exometabolite pools in either the day or night ($p < 0.05$; random effect of subnetwork). Among those with differential organismal production, roughly half again (Quinlan et al. 2019) differed significantly between the exudates of fleshy algae and corals ($p < 0.05$; random effect of subnetwork and organism). To visualise how these widespread labile compounds are enriched among different producers, we used hierarchical clustering (Figure 5c) to qualitatively organise relative enrichment or depletion of the most abundant and significant annotated labile exometabolite subclasses. The clustering pattern reiterates and illuminates the ordination patterns in Figure 5a, demonstrating three clear clusters of labile exometabolite pools: coral exudates, nighttime algal exudates and daytime algal exudates. The coral exudates are defined by the enrichment of fatty acyls (fatty acid esters and linoleic acids), carboxylic acids and glycerophosphoethanolamines. The nighttime algal exudates are enriched in diterpenoids, peptides and additional types of fatty acyls (including fatty amides), while in the daytime, algal exudates are enriched in prenol lipids, amines and two types of organoheterocyclic compounds (indoles and triazines).

4 | Discussion

Characterising the DOM pool, specifically the labile portion, has proven to be exceptionally difficult due to the short residence time of labile carbon sources (Cherrier et al. 1996; Carlson et al. 2004, 2002). Because of this rapid degradation,

the detection of labile DOM in nature is often entirely missed, and instead, we only observe the effects of its consumption (e.g., microbially sourced metabolites, microbial community composition; 5). To our knowledge, this is the first study to employ untargeted tandem mass spectrometry to broadly characterise labile compounds within the marine DOM pool. Our DOM dilution culture experiment showed that labile compounds released by coral reef primary producers were not limited to a few chemical families but rather included representation across 8 of the 16 superclass categories (Figures 1 and S5). Moreover, exudation of labile DOM from these categories differed day and night by benthic producer: both coral and fleshy algae released more bioavailable lipids and organic nitrogen compounds at night, *Dictyota* algae produced higher intensities of labile organic acids during the day, while both fleshy algae and *Porites* released higher intensities of labile heterocyclic compounds during day 1 (Figure 2). By linking metabolite utilisation with microbial community growth, our study further showed that coral-derived labile exometabolites enhanced specific growth rates both day and night, while algae-derived labile metabolites had a significant impact on microbial growth during the day but not at night (Figures 3 and S3). These effects translated to the degree of selection in microbial communities, with daytime algal exudates imposing stronger selection (reduced evenness) and coral exudates more selective at night, enriching a single Rhodobacteraceae OTU (Figures 4 and S4). Our study describes how coral reef primary producers selectively facilitate the growth of specific heterotrophic microbial communities through the exudation of structurally distinct labile exometabolites (Figures 2 and 5) that are subsequently transformed during microbial metabolism (Figures 3 and 4). This work can thus guide the generation of future hypotheses about key compounds that drive the microbial carbon cycle in aquatic ecosystems (Moran et al. 2016).

Consistent with previous work (Wegley Kelly et al. 2022), roughly one-quarter of the ion features found in this untargeted analysis of seawater around coral reef benthic primary producers were defined as exometabolites, with each organism releasing more than 400 distinct compounds. This emphasises the key role of benthic producers in coastal ecosystems and their contribution to the organic carbon pool. Untargeted approaches have great potential to complement targeted quantification of exometabolites (Weber et al. 2022) by expanding the diversity and complexity of the chemical ecology of these critical ecosystems (Nelson et al. 2013; Weber et al. 2020). Using machine learning algorithms to predict structural characteristics of molecular families (Dührkop et al. 2021), we additionally documented clear patterns in the types of compounds released by different coral reef producers, demonstrating that most exudates were mainly lipids and organic acids, with significant portions of heterocyclics, benzenoids and organic oxygen and nitrogen compounds but with clear biases: corals tended to release more labile lipids (both day and night) and algae more heterocyclics during the day. We expanded this further by demonstrating that all reef organisms increased the production of lipids and organic nitrogen compounds and reduced the production of heterocyclics at night, generating new hypotheses about diel shifts in coral reef microbial ecosystems.

This study further expands on this concept by demonstrating that a significant fraction of these exometabolites are labile: roughly half of the total amount and diversity of exometabolites released by benthic organisms belong to labile molecular families in both the day and night. This reinforces the emerging view of freshly produced DOM as being largely labile and rapidly metabolised by microbial communities (Goldberg et al. 2017; Romera-Castillo et al. 2011) and provides a quantitative structural framework for how consistent this proportion is across diverse phyla of benthic primary producers. Crucially, our study demonstrates that at least 15% of the compounds in each superclass category of the ChemOnt found in this study are labile, suggesting that lability is not constrained only to specific types of compounds or size classes as is commonly thought (Benner and Amon 2015). The specific compound classes comprising the labile DOM pool are largely unknown, though several studies have predicted putative labile compounds based on genetic information about transporters and catabolic enzymes (McCarren et al. 2010; Poretsky et al. 2010; Gifford et al. 2013; Lidbury et al. 2014; Durham et al. 2015; Liu et al. 2015). For example, carboxylic acids, alcohols and carbohydrates have all been proposed as labile substrates (Poretsky et al. 2010; Gifford et al. 2013). Our results are consistent with these prior studies, illustrating a significant drawdown of exometabolites putatively classified as carbohydrates, carboxylic acids and fatty acyls, and additionally we identified several putative triazenes, indoles, prenol lipids and glycerophospholipids that appear labile (Figures 5 and S4).

Because of the solid-phase extraction required for DOM characterisation, hydrophobic classes such as lipids and lipid-like compounds were the most prevalent chemical entities annotated within our datasets and comprised one of the primary classes of labile compounds identified (Figure 2b,c). Fatty acids have been proposed as putatively labile structures based on microbial expression studies (McCarren et al. 2010), and our study found that a total of nine putative fatty acid subnetworks were bioavailable. Six of these fatty acid subnetworks were produced by at least one of the algae within our experiment, and the other three were either cosmopolitan or produced by reef-builders (Figure S4). A particularly large extent of fatty acyl compounds including fatty acid esters and linoleic acids comprised a major fraction of the exometabolites produced and utilised from corals, consistent with previous documentation of their presence in exudate pools (Wegley Kelly et al. 2022) and tissues (Mannochio-Russo et al. 2023), while fatty amides tended to be labile exometabolites of fleshy algae. Several other lipid categories were labile, including prenol lipids, glycerophospholipids, ceramides and steroids (Figure S4). The prenol lipids and its subclasses, diterpenoids and terpene lactones, were almost exclusively produced by fleshy algae (Figures 5 and S4), demonstrating the lability of these compounds previously shown to be released by macroalgae (Wegley Kelly et al. 2022). Overall, the glycerophospholipids and steroids were produced by all five organisms, consistent with their dominance in tissue metabolomes of diverse coral reef organisms (Mannochio-Russo et al. 2023), while the ceramides were only exuded by CCA and *Porites* corals. Other unexpected labile classes include heterocyclic compounds and benzenoids as these ring structures are theoretically difficult to degrade (Lu et al. 2018; Krylov and Mamontov 2022). These data suggest that the breadth of labile compounds is larger than those previously described within the biochemical pathways of specific marine microbes (McCarren et al. 2010; Pontiller et al. 2020). Finally,

our results reinforce the idea that untargeted mass spectrometry can expand the current understanding about the interplay between DOM composition and biological lability by identifying new labile compound classes.

Characterisations of DOM pools in the ocean are hindered twofold: first, an untargeted approach identifies thousands of unknown ion features, providing limited annotation rates for previously unidentified spectra (Moran et al. 2016; Koester et al. 2022; Wegley Kelly et al. 2021); and second, the solid-phase extraction methodology has a strong affinity for non-polar, hydrophobic molecules, biasing the DOM composition against certain compound classes, such as carbohydrates (Johnson et al. 2017). Consistent with the first limitation, less than 10% of our DOM features matched spectral databases. To expand structural predictions of DOM features, we employed the machine learning tool CANOPUS followed by ConCISE subnetwork consensus, which raised our putative annotation rate to 53.6%. As spectral libraries grow and predictive algorithms are improved, we anticipate that the field will gain higher confidence in these cheminformatic approaches (Dührkop et al. 2021; Quinlan et al. 2022). In addition, newer advancements such as a derivatisation method that has been shown to enhance the detectability of structurally diverse functional groups will expand the current compositional biases from predominantly non-polar and hydrophobic molecules (Widner et al. 2021). Because of these *analytical blind spots*, we likely missed relevant labile exometabolites produced by fleshy algae treatments during the daytime, such as dissolved combined neutral sugars, which have previously shown to be produced by fleshy algae (Nelson et al. 2013). Furthermore, while the experimental design reduced microbial consumption of labile exometabolites by 0.2-μm filtering the seawater during exudate capture, it was not possible to eliminate the activity of organism-associated microbes. Finally, this studied untargeted approach enabled the experimental identification of labile metabolite chemodiversity past those that have been previously predicted but cannot quantify the fluxes in metabolite concentration (e.g., μm). This provides the opportunity for future studies to target specific labile metabolites identified herein and quantify their concentration and carbon flux.

Coral reef ecosystems are degrading worldwide by a process referred to as *microbialisation* (Haas et al. 2016; McDole et al. 2012). The mechanism driving this microbialisation process is posited to involve labile DOM released by fleshy algae, which engenders higher microbial standing stocks and populations of microbial taxa that harness copiotrophic feeding strategies, resulting in higher coral disease prevalence and mortality (Haas et al. 2016; Dinsdale et al. 2008; Barott and Rohwer 2012; Silveira et al. 2017). Daytime exudates of fleshy algae engendered higher microbial loads (Figure S2) and selected for genera such as *Nautella* and *Donghicola* (Figure 4, Table S2) that exhibit moderately copiotrophic feeding strategies (Pujalte et al. 2014; Meyer et al. 2019; Rosales et al. 2019). In contrast, daytime coral exudates selected for more oligotrophic guilds (Nelson et al. 2013; Brown et al. 2009) such as *Prochlorococcus*, NS9 marine group (Flavobacteriales) *and* OM60 (Halieaceae) (Figure 4, Table S2). Importantly, the growth of microbial communities on coral exudates was more tightly coupled to the utilisation of labile exometabolites in the daytime than growth on algal exudates, suggesting that the rapid enhancement of bacterial growth on algal exudates was driven by compounds outside of our analytical window such as oligosaccharides (Nelson et al. 2013).

These daytime results support prior studies on microbial responses to algal exudates (Nelson et al. 2013; Haas et al. 2013, 2011), but achieving a mechanistic understanding of microbialisation requires knowledge about how benthic primary producers influence biochemical fluxes and microbial growth patterns over the diel cycle. Only recently have studies begun characterising the microbial ecology of reefs at night, which showed drastic shifts in the microbial community structure of the reef waters (Wegley Kelly et al. 2019) and the regulation of energy metabolism within the coral holobiont (Linsmayer et al. 2020). We predict that benthic shifts in energy metabolism and metabolite fluxes influence the exudation of different labile exometabolites at night, which select for distinct microbial communities. In the present work, *Pocillopora* coral released the most labile metabolites in terms of both magnitude (Figures 2, 3 and S4) and diversity (Figures 5 and S4) at night, subsequently enriching for the highest microbial growth rates of any nighttime treatment. In both coral treatments, labile exometabolites enriched for less diverse microbial populations dominated by a single unclassified Rhodobacteraceae (64.4% and 73.9% abundance in *Porites* and *Pocillopora*; Figures 4 and 6, Table S2). This coral-selected Rhodobacteraceae taxon was never enriched by algal exometabolites, although several other taxa from the same family were enhanced at night in the fleshy algae treatments (Figure 4).

Compared to both corals, the fleshy algae exometabolites produced at night had less impact on their microbial communities in terms of both microbial growth and community composition (Figure 6). Additionally, labile exometabolites were both produced and depleted with greater magnitude at night in the coral treatments (*Pocillopora* and *Porites*; FDR $p < 0.01$ and $p < 0.0393$; Figures 3a and 6). There was no significant diel change in either the production or depletion of fleshy algal labile exometabolites (*Dictyota* and Turf; $p > 0.05$). The dichotomy in nighttime labile exometabolite production between corals and fleshy algae was not expected, although it makes sense biologically since fleshy algae rely entirely upon photosynthesis for energy acquisition, whereas corals can feed heterotrophically day and night to supplement their energetic demands (Houlbrèque and Ferrier-Pagès 2009; Chen et al. 2013). It is also likely that in natural habitats, the microbial communities enriched by *Pocillopora* would exhibit lower concentrations because coral heterotrophy directly consumes them (Houlbrèque and Ferrier-Pagès 2009), and this ecological influence represents another limitation within our experimental design.

To conclude, our study characterises novel labile exometabolites derived from coral reef environments, illustrating large differences in the quantity and diversity of organic substrates produced by benthic primary producers. At night, corals maintained similar microbial growth rates through the consistent production of labile substrates, whereas fleshy algae reduced the exudation of labile compounds during the night, providing fewer energetic substrates to microbes at this time. This finding reveals an enigmatic twist to understanding the mechanisms underlying coral reef microbialisation and warrants further investigation. Our study further highlights the potential of untargeted metabolomics to expand the understanding of microbial

interactions with diverse types of bioavailable DOM and unravel the structural dynamics underpinning the lability of dissolved organic matter.

Author Contributions

Zachary A. Quinlan: conceptualization, investigation, funding acquisition, writing – original draft, methodology, visualization, writing – review and editing, formal analysis, data curation. **Craig E. Nelson:** conceptualization, investigation, funding acquisition, writing – original draft, methodology, formal analysis, data curation, supervision, resources, writing – review and editing. **Irina Koester:** investigation, writing – review and editing, methodology, data curation. **Daniel Petras:** investigation, writing – review and editing, data curation. **Louis-Felix Nothias:** writing – review and editing, investigation, data curation. **Jacqueline Comstock:** writing – review and editing, investigation, data curation. **Brandie M. White:** investigation, data curation, writing – review and editing. **Lihini I. Aluwihare:** investigation, resources, writing – review and editing, funding acquisition. **Barbara A. Bailey:** writing – review and editing, data curation, formal analysis. **Craig A. Carlson:** writing – review and editing, data curation, investigation, funding acquisition. **Pieter C. Dorrestein:** funding acquisition, writing – review and editing, resources, supervision. **Andreas F. Haas:** resources, data curation, writing – review and editing, investigation. **Linda Wegley Kelly:** supervision, resources, data curation, writing – review and editing, investigation, funding acquisition, conceptualization, formal analysis.

Acknowledgements

We thank Adi Khen for the use of her graphics of corals and algae, Bryce Inman for help in designing the experimental graphic and Forest Rohwer for providing guidance, lab space and unwavering criticism. This research was sponsored by the US National Science Foundation awards OCE-2118617 and OCE-2118618 to L.W.K., OCE-2023298 to C.E.N. and OCE-2023509 to L.I.A. and P.C.D. in collaboration with the Moorea Coral Reef Long-Term Ecological Research project (MCR-LTER; OCE-1637396). Z.A.Q. was additionally funded by the US National Science Foundation (GRFP-2019252845). This research was also funded in part by a grant/cooperative agreement from the National Oceanic and Atmospheric Administration, Project A/AS-1; which is sponsored by the University of Hawaii Sea Grant College Program, School of Ocean and Earth Science and Technology (SOEST), under Institutional Grant No., NA24OARX417C0024-T1-01 from NOAA Office of Sea Grant, Department of Commerce. The views expressed herein are those of the author(s) and do not necessarily reflect the views of NOAA or any of its subagencies. This is Hawaii Sea Grant publication number 4949 and SOEST grant number 11904.

Conflicts of Interest

The authors declare no conflicts of interest.

Data Availability Statement

All data from this study will be openly available upon acceptance. Biochemical data are deposited in BCO-DMO under/project/855067; Sequence data is assessible from NCBI under the bio project assession PRJNA1226244. Raw mzml for metabolomic analysis is available from the MASSIVE accession MSV000082083. All data and codes used to analyse the data are available on Github (Github.com/zquinlan/DielReefEnrichments; doi:10.5281/zenodo.7953548).

References

Ammerman, J., J. Fuhrman, A. Hagström, and F. Azam. 1984. "Bacterioplankton Growth in Seawater: I. Growth Kinetics and Cellular Characteristics in Seawater Cultures." *Marine Ecology Progress Series Oldendorf* 18, no. 1: 31–39.

Apprill, A., H. Holm, A. E. Santoro, et al. 2021. "Microbial Ecology of Coral-Dominated Reefs in the Federated States of Micronesia." *Aquatic Microbial Ecology* 86: 115–136.

Arisdakessian, C., S. B. Cleveland, and M. Belcaid. 2020. "MetaFlow|Mics: Scalable and Reproducible Nextflow Pipelines for the Analysis of Microbiome Marker Data." In *Practice and Experience in Advanced Research Computing*, 120–124. Association for Computing Machinery.

Aron, A. T., E. C. Gentry, K. L. McPhail, et al. 2020. "Reproducible Molecular Networking of Untargeted Mass Spectrometry Data Using GNPS." *Nature Protocols* 15, no. 6: 1954–1991.

Azam, F., and F. Malfatti. 2007. "Microbial Structuring of Marine Ecosystems." *Nature Reviews Microbiology* 5, no. 10: 782–791.

Barott, K. L., and F. L. Rohwer. 2012. "Unseen Players Shape Benthic Competition on Coral Reefs." *Trends in Microbiology* 20, no. 12: 621–628.

Benjamini, Y., and Y. Hochberg. 1995. "Controlling the False Discovery Rate: A Practical and Powerful Approach to Multiple Testing." *Journal of the Royal Statistical Society* 57: 1–13.

Benner, R., and R. M. W. Amon. 2015. "The Size-Reactivity Continuum of Major Bioelements in the Ocean." *Annual Review of Marine Science* 7, no. 1: 185–205.

Brocke, H. J., F. Wenzhoefer, D. de Beer, B. Mueller, F. C. van Duyl, and M. M. Nugues. 2015. "High Dissolved Organic Carbon Release by Benthic Cyanobacterial Mats in a Caribbean Reef Ecosystem." *Scientific Reports* 5, no. 1: 8852.

Brown, M. V., G. K. Philip, J. A. Bunge, et al. 2009. "Microbial Community Structure in the North Pacific Ocean." *ISME Journal* 3, no. 12: 1374–1386.

Callahan, B. J., J. Wong, C. Heiner, et al. 2019. "High-Throughput Amplicon Sequencing of the Full-Length 16S rRNA Gene With Single-Nucleotide Resolution." *Nucleic Acids Research* 47, no. 18: e103.

Carlson, C., S. Giovannoni, D. Hansell, et al. 2002. "Effect of Nutrient Amendments on Bacterioplankton Production, Community Structure, and DOC Utilization in the Northwestern Sargasso Sea." *Aquatic Microbial Ecology* 30: 19–36.

Carlson, C. A., S. J. Giovannoni, D. A. Hansell, S. J. Goldberg, R. Parsons, and K. Vergin. 2004. "Interactions Among Dissolved Organic Carbon, Microbial Processes, and Community Structure in the Mesopelagic Zone of the Northwestern Sargasso Sea." *Limnology and Oceanography* 49, no. 4: 1073–1083.

Carlson, C. A., and D. A. Hansell. 2014. "DOM Sources, Sinks, Reactivity, and Budgets." In *Biogeochemistry of Marine Dissolved Organic Matter*, edited by D. A. Hansell and C. A. Carlson, 65–126. Elsevier.

Chen, C.-Y., X.-Q. Zhao, H.-W. Yen, et al. 2013. "Microalgae-Based Carbohydrates for Biofuel Production." *Biochemical Engineering Journal* 78: 1–10.

Cherrier, J., J. Bauer, and E. Druffel. 1996. "Utilization and Turnover of Labile Dissolved Organic Matter by Bacterial Heterotrophs in Eastern North Pacific Surface Waters." *Marine Ecology Progress Series* 139: 267–279.

Dick, J. M. 2019. "CHNOSZ: Thermodynamic Calculations and Diagrams for Geochemistry." *Frontiers in Earth Science* 7: 180.

Dinsdale, E. A., O. Pantos, S. Smriga, et al. 2008. "Microbial Ecology of Four Coral Atolls in the Northern Line Islands." *PLoS One* 3, no. 2: e1584.

Dittmar, T., B. Koch, N. Hertkorn, and G. Kattner. 2008. "A Simple and Efficient Method for the Solid-Phase Extraction of Dissolved Organic Matter (SPE-DOM) From Seawater." *Limnology and Oceanography: Methods* 6, no. 6: 230–235.

Dixon, P. 2003. "VEGAN, a Package of R Functions for Community Ecology." *Journal of Vegetation Science* 14, no. 6: 927–930.

Djoumbou Feunang, Y., R. Eisner, C. Knox, et al. 2016. "ClassyFire: Automated Chemical Classification With a Comprehensive, Computable Taxonomy." *Journal of Cheminformatics* 8, no. 1: 61.

Dowle, M., A. Srinivasan, J. Gorecki, et al. 2019. "Package 'data.table'. Extension of 'Data.Frame." *R Package* version 1: 6.

Duarte, C. M., and J. Cebrián. 1996. "The Fate of Marine Autotrophic Production." *Limnology and Oceanography* 41, no. 8: 1758–1766.

Dührkop, K., L.-F. Nothias, M. Fleischauer, et al. 2021. "Systematic Classification of Unknown Metabolites Using High-Resolution Fragmentation Mass Spectra." *Nature Biotechnology* 39, no. 4: 462–471.

Durham, B. P., S. Sharma, H. Luo, et al. 2015. "Cryptic Carbon and Sulfur Cycling Between Surface Ocean Plankton." *National Academy of Sciences of the United States of America* 112, no. 2: 453–457.

Gifford, S. M., S. Sharma, M. Booth, and M. A. Moran. 2013. "Expression Patterns Reveal Niche Diversification in a Marine Microbial Assemblage." *ISME Journal* 7, no. 2: 281–298.

Glasl, B., D. G. Bourne, P. R. Frade, T. Thomas, B. Schaffelke, and N. S. Webster. 2019. "Microbial Indicators of Environmental Perturbations in Coral Reef Ecosystems." *Microbiome* 7, no. 1: 94.

Goldberg, S. J., C. E. Nelson, D. A. Viviani, C. N. Shulse, and M. J. Church. 2017. "Cascading Influence of Inorganic Nitrogen Sources on DOM Production, Composition, Lability and Microbial Community Structure in the Open Ocean." *Environmental Microbiology* 19, no. 9: 3450–3464.

Haas, A. F., M. F. M. Fairoz, L. W. Kelly, et al. 2016. "Global Microbialization of Coral Reefs." *Nature Microbiology* 1: 16042.

Haas, A. F., C. E. Nelson, F. Rohwer, et al. 2013. "Influence of Coral and Algal Exudates on Microbially Mediated Reef Metabolism." *PeerJ* 1, no. 11: e108.

Haas, A. F., C. E. Nelson, L. Wegley Kelly, et al. 2011. "Effects of Coral Reef Benthic Primary Producers on Dissolved Organic Carbon and Microbial Activity." *PLoS One* 6, no. 11: e27973.

Hagström, A., J. Ammerman, S. Henrichs, and F. Azam. 1984. "Bacterioplankton Growth in Seawater: II. Organic Matter Utilization During Steady-State Growth in Seawater Cultures." *Marine Ecology Progress Series Oldendorf* 18, no. 1: 41–48.

Hansell, D. A. 2013. "Recalcitrant Dissolved Organic Carbon Fractions." *Annual Review of Marine Science* 5, no. 1: 421–445.

Houlbrèque, F., and C. Ferrier-Pagès. 2009. "Heterotrophy in Tropical Scleractinian Corals." *Biological Reviews* 84, no. 1: 1–17.

Jani, A. J., J. Bushell, C. G. Arisdakessian, et al. 2021. "The Amphibian Microbiome Exhibits Poor Resilience Following Pathogen-Induced Disturbance." *ISME Journal* 15, no. 6: 1628–1640.

Johnson, W. M., M. C. Kido Soule, and E. B. Kujawinski. 2017. "Extraction Efficiency and Quantification of Dissolved Metabolites in Targeted Marine Metabolomics." *Limnology and Oceanography: Methods* 15, no. 4: 417–428.

Kassambara, A., and M. A. Kassambara. 2020. "Package 'ggpubr'. R Package Version 01." 6(0).

Klindworth, A., E. Pruesse, T. Schweer, et al. 2012. "Evaluation of General 16S Ribosomal RNA Gene PCR Primers for Classical and Next-Generation Sequencing-Based Diversity Studies." *Nucleic Acids Research* 41, no. 1: e1.

Koester, I., Z. A. Quinlan, L. F. Nothias, et al. 2022. "Illuminating the Dark Metabolome of Pseudo-Nitzschia-Microbiome Associations." *Environmental Microbiology* 24, no. 11: 5408–5424.

Kozich, J. J., S. L. Westcott, N. T. Baxter, S. K. Highlander, and P. D. Schloss. 2013. "Development of a Dual-Index Sequencing Strategy and Curation Pipeline for Analyzing Amplicon Sequence Data on the MiSeq Illumina Sequencing Platform." *Applied and Environmental Microbiology* 79, no. 17: 5112–5120.

Krylov, V. A., and V. G. Mamontov. 2022. "The Impact of Different Cenoses on the Thermal Characteristics of Labile Humic Substances of Typical Chernozem in Kursk Oblast." *Eurasian Soil Science* 55, no. 4: 452–459.

Lidbury, I., J. C. Murrell, and Y. Chen. 2014. "Trimethylamine N—Oxide Metabolism by Abundant Marine Heterotrophic Bacteria." *National Academy of Sciences of the United States of America* 111, no. 7: 2710–2715.

Linsmayer, L. B., D. D. Deheyn, L. Tomanek, and M. Tresguerres. 2020. "Dynamic Regulation of Coral Energy Metabolism Throughout the Diel Cycle." *Scientific Reports* 10, no. 1: 19881.

Liu, Q., X. Lu, B. B. Tolar, X. Mou, and J. T. Hollibaugh. 2015. "Concentrations, Turnover Rates and Fluxes of Polyamines in Coastal Waters of the South Atlantic Bight." *Biogeochemistry* 123, no. 1–2: 117–133.

Lu, D., F. Sun, and Y. Zhou. 2018. "Insights Into Anaerobic Transformation of Key Dissolved Organic Matters Produced by Thermal Hydrolysis Sludge Pretreatment." *Bioresource Technology* 266: 60–67.

Ludwig, M., K. Dührkop, and S. Böcker. 2018. "Bayesian Networks for Mass Spectrometric Metabolite Identification via Molecular Fingerprints." *Bioinformatics* 34, no. 13: i333–i340.

Ludwig, M., L.-F. Nothias, K. Dührkop, et al. 2020. "Database-Independent Molecular Formula Annotation Using Gibbs Sampling Through ZODIAC." *Nature Machine Intelligence* 2, no. 10: 629–641.

Mannochio-Russo, H., S. O. Swift, K. K. Nakayama, et al. 2023. "Microbiomes and Metabolomes of Dominant Coral Reef Primary Producers Illustrate a Potential Role for Immunolipids in Marine Symbioses." *Communications Biology* 6, no. 1: 896.

Mao-Jones, J., K. B. Ritchie, L. E. Jones, and S. P. Ellner. 2010. "How Microbial Community Composition Regulates Coral Disease Development." *PLoS Biology* 8, no. 3: e1000345.

McCarren, J., J. W. Becker, D. J. Repeta, et al. 2010. "Microbial Community Transcriptomes Reveal Microbes and Metabolic Pathways Associated With Dissolved Organic Matter Turnover in the Sea." *National Academy of Sciences of the United States of America* 107, no. 38: 16420–16427.

McDole, T., J. Nulton, K. L. Barott, et al. 2012. "Assessing Coral Reefs on a Pacific-Wide Scale Using the Microbialization Score." *PLoS One* 7, no. 9: e43233.

Meyer, J. L., J. Castellanos-Gell, G. S. Aeby, C. C. Häse, B. Ushijima, and V. J. Paul. 2019. "Microbial Community Shifts Associated With the Ongoing Stony Coral Tissue Loss Disease Outbreak on the Florida Reef Tract." *Frontiers in Microbiology* 10: 2244.

Moran, M. A., E. B. Kujawinski, A. Stubbins, et al. 2016. "Deciphering Ocean Carbon in a Changing World." *National Academy of Sciences of the United States of America* 113, no. 12: 3143–3151.

Mueller, B., H. J. Brocke, F. L. Rohwer, et al. 2022. "Nocturnal Dissolved Organic Matter Release by Turf Algae and Its Role in the Microbialization of Reefs." *Functional Ecology* 36, no. 8: 2104–2118.

Nelson, C. E., M. J. Donahue, H. Dulaiova, et al. 2015. "Fluorescent Dissolved Organic Matter as a Multivariate Biogeochemical Tracer of Submarine Groundwater Discharge in Coral Reef Ecosystems." *Marine Chemistry* 177: 1–12.

Nelson, C. E., S. J. Goldberg, L. W. Kelly, et al. 2013. "Coral and Macroalgal Exudates Vary in Neutral Sugar Composition and Differentially Enrich Reef Bacterioplankton Lineages." *ISME Journal* 7, no. 5: 962–979.

Nelson, C. E., L. Wegley Kelly, and A. F. Haas. 2023. "Microbial Interactions With Dissolved Organic Matter Are Central to Coral Reef

Ecosystem Function and Resilience." *Annual Review of Marine Science* 15: 431–460.

Neuwirth, E., and M. E. Neuwirth. 2011. "Package 'RColorBrewer'." *Physical Review D: Particles, Fields, Gravitation, and Cosmology* 84: 1–5.

Nothias, L.-F., D. Petras, R. Schmid, et al. 2020. "Feature-Based Molecular Networking in the GNPS Analysis Environment." *Nature Methods* 17, no. 9: 905–908.

Paradis, E., J. Claude, and K. Strimmer. 2004. "APE: Analyses of Phylogenetics and Evolution in R Language." *Bioinformatics* 20, no. 2: 289–290.

Petras, D., I. Koester, R. Da Silva, et al. 2017. "High-Resolution Liquid Chromatography Tandem Mass Spectrometry Enables Large Scale Molecular Characterization of Dissolved Organic Matter. Frontiers in Marine." *Science* 4: 4.

Pluskal, T., S. Castillo, A. Villar-Briones, and M. Orešič. 2010. "MZmine 2: Modular Framework for Processing, Visualizing, and Analyzing Mass Spectrometry-Based Molecular Profile Data." *BMC Bioinformatics* 11, no. 1: 395.

Pontiller, B., S. Martínez-García, D. Lundin, and J. Pinhassi. 2020. "Labile Dissolved Organic Matter Compound Characteristics Select for Divergence in Marine Bacterial Activity and Transcription." *Frontiers in Microbiology* 11: 588778.

Poretsky, R. S., S. Sun, X. Mou, and M. A. Moran. 2010. "Transporter Genes Expressed by Coastal Bacterioplankton in Response to Dissolved Organic Carbon." *Environmental Microbiology* 12, no. 3: 616–627.

Pujalte, M. J., T. Lucena, M. A. Ruvira, D. R. Arahal, and M. C. Macián. 2014. *The Family Rhodobacteraceae*, 439–512. Springer Berlin Heidelberg.

Quinlan, Z. A., I. Koester, A. T. Aron, et al. 2022. "ConCISE: Consensus Annotation Propagation of Ion Features in Untargeted Tandem Mass Spectrometry Combining Molecular Networking and In Silico Metabolite Structure Prediction." *Metabolites* 12, no. 12: 1275.

Quinlan, Z. A., K. Remple, M. D. Fox, et al. 2018. "Fluorescent Organic Exudates of Corals and Algae in Tropical Reefs Are Compositionally Distinct and Increase With Nutrient Enrichment." *Limnology and Oceanography Letters* 3, no. 4: 331–340.

Quinlan, Z. A., R. Ritson-Williams, B. J. Carroll, C. A. Carlson, and C. E. Nelson. 2019. "Species-Specific Differences in the Microbiomes and Organic Exudates of Crustose Coralline Algae Influence Bacterioplankton Communities." *Frontiers in Microbiology* 10: 2397.

Repeta, D. J., and Aluwihare. 2024. "Chemical Characterization and Cycling of Dissolved Organic Matter." In *Biogeochemistry of Marine Dissolved Organic Matter*, edited by D. A. Hansell and C. A. Carlson, 13–67. Elsevier.

Roach, T. N., M. L. Abieri, E. E. George, et al. 2017. "Microbial Bioenergetics of Coral-Algal Interactions." *PeerJ* 5: e3423.

Rognes, T., T. Flouri, B. Nichols, C. Quince, and F. Mahé. 2016. "VSEARCH: A Versatile Open Source Tool for Metagenomics." *PeerJ* 4: e2584.

Romera-Castillo, C., H. Sarmento, X. A. Alvarez-Salgado, J. M. Gasol, and C. Marrasé. 2011. "Net Production and Consumption of Fluorescent Colored Dissolved Organic Matter by Natural Bacterial Assemblages Growing on Marine Phytoplankton Exudates." *Applied and Environmental Microbiology* 77, no. 21: 7490–7498.

Rosales, S. M., M. W. Miller, D. E. Williams, N. Traylor-Knowles, B. Young, and X. M. Serrano. 2019. "Microbiome Differences in Disease-Resistant vs. Susceptible Acropora Corals Subjected to Disease Challenge Assays." *Scientific Reports* 9, no. 1: 18279.

Schloss, P. D., S. L. Westcott, T. Ryabin, et al. 2009. "Introducing Mothur: Open-Source, Platform-Independent, Community-Supported Software for Describing and Comparing Microbial Communities." *Applied and Environmental Microbiology* 75, no. 23: 7537–7541.

Schmid, R., D. Petras, L.-F. Nothias, et al. 2021. "Ion Identity Molecular Networking for Mass Spectrometry-Based Metabolomics in the GNPS Environment." *Nature Communications* 12, no. 1: 3832.

Signorell, A., K. Aho, A. Alfons, et al. 2019. "DescTools: Tools for Descriptive Statistics. R Package Version 099." 28:17.

Silveira, C. B., G. S. Cavalcanti, J. M. Walter, et al. 2017. "Microbial Processes Driving Coral Reef Organic Carbon Flow." *FEMS Microbiology Reviews* 41, no. 4: 575–595.

Smith, J. E., M. Shaw, R. A. Edwards, et al. 2006. "Indirect Effects of Algae on Coral: Algae-Mediated, Microbe-Induced Coral Mortality." *Ecology Letters* 9, no. 7: 835–845.

Wang, M., J. J. Carver, V. V. Phelan, et al. 2016. "Sharing and Community Curation of Mass Spectrometry Data With Global Natural Products Social Molecular Networking." *Nature Biotechnology* 34, no. 8: 828–837.

Weber, L., P. González-Díaz, M. Armenteros, et al. 2020. "Microbial Signatures of Protected and Impacted Northern Caribbean Reefs: Changes From Cuba to the Florida Keys." *Environmental Microbiology* 22, no. 1: 499–519.

Weber, L., M. K. Soule, K. Longnecker, et al. 2022. "Benthic Exometabolites and Their Ecological Significance on Threatened Caribbean Coral Reefs." *ISME Communications* 2, no. 1: 101.

Wegley Kelly, L., C. E. Nelson, L. I. Aluwihare, et al. 2021. "Molecular Commerce on Coral Reefs: Using Metabolomics to Reveal Biochemical Exchanges Underlying Holobiont Biology and the Ecology of Coastal Ecosystems." *Frontiers in Marine Science* 8, no. 969: 630799.

Wegley Kelly, L., C. E. Nelson, A. F. Haas, et al. 2019. "Diel Population and Functional Synchrony of Microbial Communities on Coral Reefs." *Nature Communications* 10, no. 1: 1691.

Wegley Kelly, L., C. E. Nelson, D. Petras, et al. 2022. "Distinguishing the Molecular Diversity, Nutrient Content, and Energetic Potential of Exometabolomes Produced by Macroalgae and Reef-Building Corals." *Proceedings of the National Academy of Sciences* 119, no. 5: e2110283119.

Wegley Kelly, L., G. J. Williams, K. L. Barott, et al. 2014. "Local Genomic Adaptation of Coral Reef-Associated Microbiomes to Gradients of Natural Variability and Anthropogenic Stressors." *National Academy of Sciences of the United States of America* 111, no. 28: 10227–10232.

Wickham, H., M. Averick, J. Bryan, et al. 2019. "Welcome to the Tidyverse." *Journal of Open Source Software* 4, no. 43: 1686.

Wickham, H., J. Bryan, M. Kalicinski, et al. 2019. "Package 'readxl'. Version, 13."

Widner, B., M. C. Kido Soule, F. X. Ferrer-González, M. A. Moran, and E. B. Kujawinski. 2021. "Quantification of Amine- and Alcohol-Containing Metabolites in Saline Samples Using Pre-Extraction Benzoyl Chloride Derivatization and Ultrahigh Performance Liquid Chromatography Tandem Mass Spectrometry (UHPLC MS/MS)." *Analytical Chemistry* 93, no. 11: 4809–4817.

Supporting Information

Additional supporting information can be found online in the Supporting Information section.